Original Article

Remodeling of rat pulmonary artery induced by chronic smoking exposure

Lei Zhao[1*], Jian Wang[2*], Lu Wang[1*], Yu-Ting Liang[3], Yu-Qin Chen[2], Wen-Jun Lu[2], Wen-Liang Zhou[3]

[1]Department of Physiology, School of Basic Science, Guangzhou Medical University, Guangzhou 510182, China; [2]Guangzhou Institute of Respiratory Disease, State Key Laboratory of Respiratory Diseases, The First Affiliated Hospital of Guangzhou Medical University, Guangzhou 510120, China; [3]School of Life Science, Sun Yat-Sen University, Guangzhou 510275, China

*These authors contributed equally to this work.

Correspondence to: Lei Zhao. Department of Physiology, School of Basic Science, Guangzhou Medical University, Guangzhou 510182, China. Email: crystal-zl@163.com; Jian Wang. Guangzhou Institute of Respiratory Disease, State Key Laboratory of Respiratory Diseases, The First Affiliated Hospital of Guangzhou Medical University, Guangzhou 510120, China. Email: jianwang1986@yahoo.com.

Objective: To evaluate the dominant role in rat pulmonary artery (PA) remodeling induced by chronic smoking exposure (CSE).

Methods: Thirty-five male Sprague-Dawley (SD) rats were exposed to 36 cigarettes per day, 6 days per week, for 1, 3, or 5 months. Another 35 SD rats were sham-exposed during the same period. Hemodynamic measurement, evaluation of the right ventricular hypertrophy index (RVHI) plus right ventricle-to-weight ratio, and hematoxylin eosin staining was performed. Wall thickness, artery radius, luminal area, and total area were measured morphometrically. Western blotting assessed expression of PPAR-γ BMP4, BMPR2, and TRPC1/4/6 in the artery and lung. Store-operated calcium entry (SOCE) and $[Ca^{2+}]i$ were measured using Fura-2 as dye.

Results: Mean right ventricular pressure increased after 3 months of smoking exposure and continued to increase through 5 months. Right ventricular systolic pressure (RVSP) increased after 3 months of exposure and then stabilized. RVHI increased after 5 months; right ventricle-to-weight ratio was elevated after 3 months and further increased after 5 months. Wall thickness-to-radius ratio does-dependently increased after 3 months through 5 months, in parallel with the decreased luminal area/total area ratio after 5 months. Other changes included the development of inflammatory responses, enlargement of the alveolar spaces, and reductions in the endothelial lining of PAs, proliferative smooth muscle cells, fibroblasts, and adventitia. Moreover, BMP4 and TRPC1/4/6 expression increased to varying degrees in the arteries and lungs of smoking-exposed animals, whereas BMPR expression and SOCE increased only in the arteries, and PPAR-γ was downregulated in both the arteries and lungs.

Conclusions: In SD rats, smoking exposure induces pulmonary vascular remodeling. The consequences of increased SOCE include increase in TRPC1/4/6, probably via augmented BMP4 expression, which also contribute to inflammatory responses in the lung. Moreover, interactions between BMP4 and PPAR-γ may play a role in preventing inflammation under normal physiological conditions.

Keywords: Pulmonary artery hypertension (PAH); smoking; remodeling

Submitted Mar 18, 2014. Accepted for publication Mar 25, 2014.
doi: 10.3978/j.issn.2072-1439.2014.03.31
View this article at: http://dx.doi.org/10.3978/j.issn.2072-1439.2014.03.31

Introduction

Pulmonary artery hypertension (PAH) is a disease affecting the precapillary pulmonary arterial bed, and it results from abnormal interactions between endothelial and smooth muscle cells, leading to a progressive narrowing of the pulmonary arteries (PAs) and their branches (1-3). PAH is a severe complication of smoking-induced chronic obstructive pulmonary disease (COPD) (4), in which pulmonary arterial remodeling and vasoconstriction play crucial roles, but the underlying pathogenic mechanisms are not fully understood.

BMP4 is a recently discovered vascular pro-inflammatory biomarker; its levels are enhanced in endothelial cells by disturbed blood flow, and it activates inflammation along with the generation of reactive oxygen species (ROS) in an endothelium-dependent manner (5), leading to endothelial cell malfunction (6,7). BMP4 was showed to induce and stimulate NADPH oxidases in endothelial cells *in vitro*, and therefore to produce superoxide, which in turn causes inflammatory responses (6). Although BMPs implement various functions, their signaling is transduced by binding with two types of serine/threonine kinase receptors, BMPRI and BMPRII (8-11).

According to Takano *et al*., modulation of the interactive BMP system and TNF-α receptor signaling essential for bone metabolism is related to the functional activities of PPAR (12). Moreover, BMP4 was previously found to augment the expression of TRPC1, TRPC4, and TRPC6 in cultured rat pulmonary arterial smooth muscle cells (PASMCs) (13).

In addition, TRPC1 and TRPC4 are likely to constitute a store-operated calcium channel (SOCC) (14-17), participating primarily in store-operated calcium entry (SOCE), while TRPC6 is a receptor-operated calcium channel (ROCC) involved in the regulation of vascular contractility (18-21). TRPC4 may contribute to the regulation of SOCE-mediated and agonist-stimulated cell proliferation and contraction of PASMCs (21-23). According to Liu *et al*., enhanced expression of TRPC1/4/6 and SOCE was observed in monocrotaline (MCT)-induced PAH (24), implying that TRPC-dependent SOCE plays a crucial role in the pathogenesis of PAH.

We, therefore, further investigated the pathogenesis of PAH by using a smoking-exposed rat model, and performed western blotting and calcium imaging to test the hypothesis that enhanced SOCE in smoking-treated arteries is involved in PPAR-γ signaling, which also plays a part in stimulating inflammatory responses that are followed by vascular remodeling.

Methods

Animals

Male SD rats (180-200 g) from the Guangdong Medical Laboratory Animal Centre were maintained in a specefic pathogen free (SPF) room providing a 12/12 light/dark cycle. The rats were acclimatized for one week before smoking exposure (25).

Smoking-exposed rat model

The smoke-exposure group consisted of 35 SD rats that were exposed to 36 commercially available non-filtered cigarettes every 12 hours (10:00-12:00 in the morning and 16:00-18:00 in the afternoon), 6 days per week, for 5 months. A further 35 SD rats in the control group were exposed to air (26,27). Rats were anesthetized with 3% pentobarbital sodium (45 mg/kg, intraperitoneal) after 1, 3, or 5 months of smoking exposure. Right ventricular systolic pressure (RVSP), right ventricular diastolic pressure (RVDP), and heart rate was measured by catheterizing the right ventricle directly with polyethylene catheters connected to pressure transducers (MP150; BIOPAC Systems. Inc., USA). After the hemodynamic measurements, the heart and lungs were removed and the ratio of the wet weight of the right ventricle to that of the left ventricular wall plus septum [RV/(LV + S)] was calculated. This is the right ventricular hypertrophy index (RVHI). The PAs were dissected as described below. All procedures were carried out according to the guidelines of the Animal Care and Use Committee of Guangzhou Medical University (24).

Isolation and culture of PASMCs

We dissected the distal (>4th generation) intrapulmonary arteries and removed the endothelium with a cotton swab. Myocytes obtained by enzymatic digestion were cultured for 4-5 days in smooth muscle growth medium (GIBCO DMEM 31600) with 10% serum in a damp atmosphere of 5% CO_2:95% air at 37 ℃. Twenty-four hours before an experiment, we exchanged the medium for some containing 0.5% serum to stop cell growth. Purity was assessed as >95% (18) by observing cell morphology under a phase-contrast microscope after immune-fluorescence staining of α-actin.

Histological staining & morphological analysis

We dissected the heart and lungs from exposed and control

rats as described above, with distal lung samples isolated for observation of remodeling in the PA and bronchus. Rats anesthetized with 3% pentobarbital sodium (45 mg/kg, intraperitoneal) were restrained in the supine position. The distal part of the left lung was removed and fixed for 24 hours in 4% paraformaldehyde, followed by embedding in paraffin wax. Six 5-μm-thick sections from each lung were stained with hematoxylin and eosin and observed and photographed using a Leica DM4000 B microscope with 20× and 40× objectives. The lumen and total area, as well as the wall thickness and arterial radii of the 51- to 150-μm (outer diameter) PAs were measured using Image Pro Plus 6.0 software (24,28).

Western blotting

PASMCs and lung specimens were lysed in radio immunoprecipitation assay lysis buffer containing 1% phenylmethanesulfonyl fluoride as a protease inhibitor, 1× PBS, 1% NP40, 0.1% SDS, 5 mM EDTA, 0.5% sodium deoxycholate, and 1 mM sodium orthovanadate. They were homogenized manually (PASMCs) or with an electric homogenizer (lung tissue). The overall protein concentration of the homogenates was quantified using bicinchoninic acid protein reagents (Bio-Rad) and bovine serum albumin standards. Protein homogenates were resolved by 10% SDS-PAGE calibrated with precision plus prestained protein molecular weight markers (Bio-Rad). Separated proteins were transferred to polyvinylidene difluoride membranes (pore size, 0.45 μm; Bio-Rad), blocked with 5% non-fat milk powder dissolved in tris-buffered saline (TBS) containing 0.2% Tween 20, and blotted with specific antibodies. Western blots were performed using rabbit anti-PPAR-ɣ (SANTA CRUZ), mouse anti-BMP4 (Millipore), mouse anti-BMPR2 (BD Transduction Laboratories), rabbit anti-TRPC1 (Alomone Labs), rabbit anti-TRPC4 (SANTA CRUZ), rabbit anti-TRPC6 (Alomone Labs), mouse anti-α-actin (SANTA CRUZ), goat anti-rabbit and goat anti-mouse IgG (KPL). The membranes were then washed five times for 10 min each and incubated with horseradish peroxidase-conjugated goat anti-rabbit or anti-mouse IgG for 70 min. Bound antibodies were detected using an Immun-Star™ WesternC™ Chemiluminescence Kit (Bio-Rad) (29).

Measurement of intracellular Ca^{2+}

SOCE and $[Ca^{2+}]_i$ were measured by dyeing with Fura-2 (Molecular Probes, Eugene, OR, USA), as previously described (18,30). The coverslips were fixed in a polycarbonate chamber clamped to a heated aluminum platform (RC-26G; Warner Instruments, Hamden, CT, USA) on the stage of a Leica DMI4000B inverted microscope. A dual channel heater controller (TC-344B; Warner Instruments) was connected to the heat exchanger to maintain its temperature at 37 ℃. Ratiometric measurement at 340 and 380 nm was performed on the Fura-2 fluorescence of single PASMCs visualized with a 20× fluorescence objective (UApo N340; Leica).

Statistical analysis

Data are shown as means ± SEM. Statistical comparisons were performed using Student's *t*-test. Differences were considered significant when $P<0.05$ (31).

Results

There were profound symptoms of PAH in smoking-exposed rats examined at the end of the 1st, 3rd, or 5th month of smoking exposure. The control animals weighed 203±3.7 g (n=21) at the start and 596±21 g (n=11) at the end of the experiment, whereas the smoke-exposed animals weighed 199±4.2 g (n=21; values not significantly different from the control group) at the start, and 472±19 g (n=10; values significantly different from the controls) at the end. RVSP significantly increased at the end of the 3rd month [control, 18.35±0.7 mmHg, n=4; chronic smoking exposure (CSE), 22.49±1.4 mmHg, n=3, $P<0.05$; *Figure 1*]. The mean RVP, calculated from the formula 1/3(RVSP - RVDP) + RVDP, also increased after three months (control, 9.06±0.63 mmHg, n=4; CSE, 12.45±0.93 mmHg, n=3, $P<0.05$), and after five months (control, 7.5±0.4 mmHg, n=5; CSE, 11.51±1.5 mmHg, n=5, $P<0.05$; *Figure 1C-G*). The RVHI RV/(LV + S) was elevated at the end of the 5th month (control, 30.54±2.32%, n=6; CSE, 43.32%±3%, n=6, $P<0.05$; *Figure 1I*), as was the RV/weight ratio (g/kg) at the end of the 3rd month (control, 0.49±0.05, n=4; CSE, 0.63±0.02, n=4, $P<0.05$) and the 5th month (control, 0.46±0.02, n=6; CSE, 0.66±0.02, n=6, $P<0.001$; *Figure 1J*).

In the histological examinations of distal lung sections of CSE rats, we observed the medial walls of the muscular small PAs (vessel outer diameters of 50-150 μm) were significantly thickened. Morphological analysis of these vessels showed the luminal area to total area ratio had significantly diminished at the end of the 5th month (control, 0.45±0.1, n=3; CSE, 0.16±0.05, n=6, $P<0.05$; *Figure 1O-Q*), and the wall thickness to artery radius ratio was notably enhanced in CSE-treated

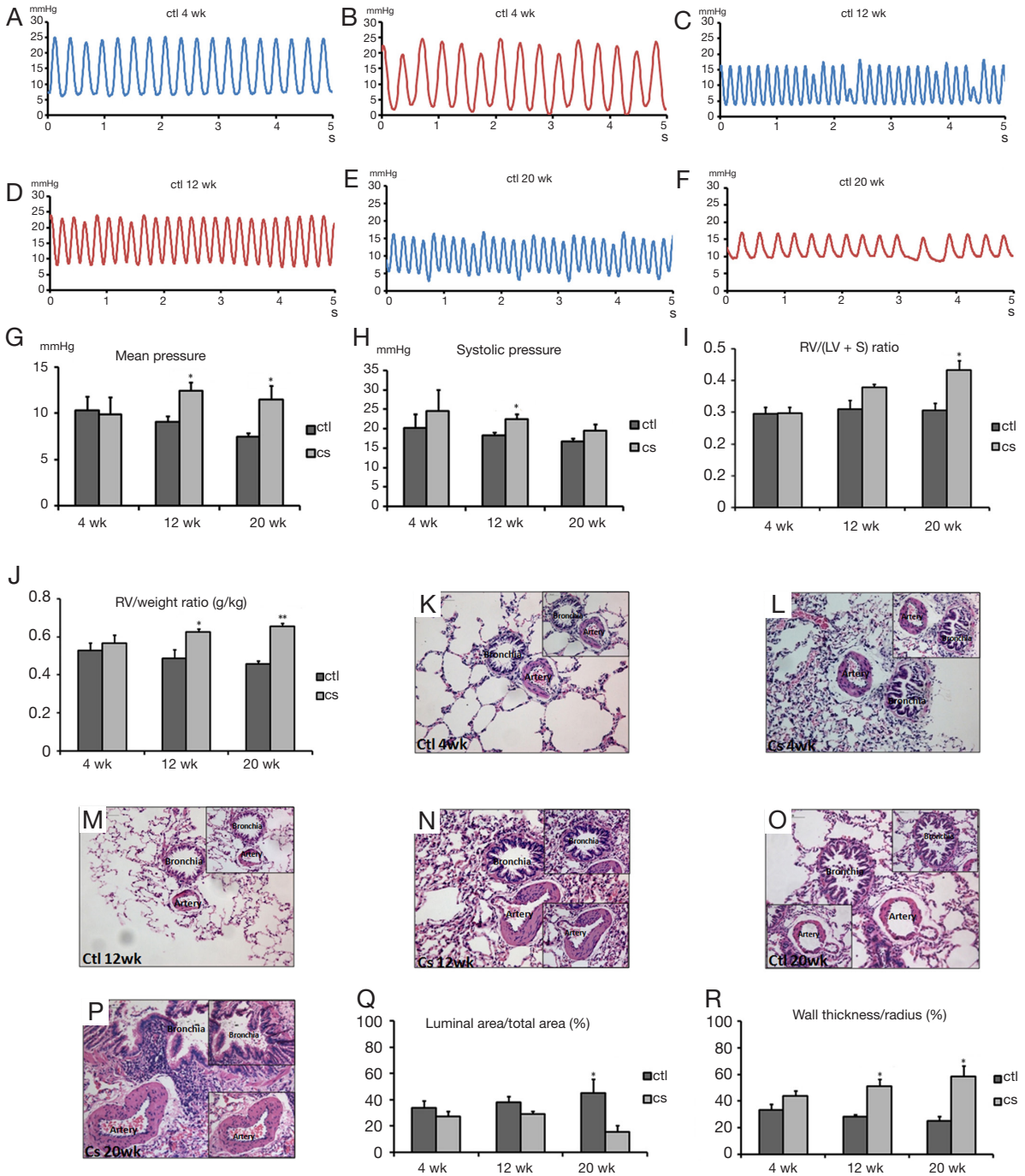

Figure 1 Verification of PAH in smoking-exposed rats. (A-F) Waveforms of representative right ventricular pressures in rats exposed to air or 4/12/20 weeks of cigarette smoke; (G,H) statistical analyses of right ventricular pressure [4-week control, n=3, 4-week chronic smoking exposure (CSE), n=5; 12-week control, n=4, 12-week CSE, n=3; 20-week control, n=5, 20-week CSE, n=5]; (I,J) RVHI, calculated as RV/(LV + S) and RV/weight (4-week control and CSE, n=4; 12-week control and CSE, n=4; 20-week control and CSE, n=6); (K-P) representative hematoxylin and eosin staining of lung slices from control and CSE rats, showing small PAs and bronchia (main photomicrographs, magnification 200×, scale bars 100 μm; small photomicrographs, magnification 400×, scale bars 50 μm); (Q,R) the ratio of luminal area to total area (%) and the ratio of wall thickness to artery radius (%) in control and CSE PAs of 51-150 μm outer diameter (4-week control and CSE, n=4; 12-week control, n=3, 12-week CSE, n=4; 20-week control, n=3, 20-week CSE, n=6). *, P value <0.05; **, P value <0.001.

rats at the end of the 3rd month (control, 0.28±0.02, n=3; CSE, 0.51±0.05, n=4, P<0.05) and the 5th month (control, 0.25±0.04, n=3; CSE, 0.58±0.08, n=6, P<0.05); these two parameters altered in a dose-dependent way (*Figure 1M-P,R*). In addition, there were the infiltration of inflammatory factors, the enlargement of the alveolar spaces, the low level of endothelial lining in the severely dilated PAs, as well as the scarcity of proliferative smooth muscle cells, fibroblasts, and adventitia (*Figure 1K-P*) (1), all of which indicate that vascular remodeling and neo-muscularization was taking place in the distal intrapulmonary arteries of rats experiencing CSE.

To further explore the molecular mechanisms underlying pulmonary vascular remodeling, SOCE and basal [Ca^{2+}] were examined at the end of five months of smoking exposure. We found that SOCE increased from 0.069±0.007 (control, n=5 in 57 cells) to 0.107±0.012 (CSE, n=5 in 87 cells; *Figure 2A,B*). The augmented SOCE in the PASMCs of rats undergoing CSE indicates that TRPC protein expression is elevated during CSE-induced PAH, as described below.

PPAR-γ protein levels (related to α-actin in endothelium-denuded PAs) declined significantly after 3 and 5 months of smoking exposure compared with the control (3 months: control, n=4; CSE, n=5, P<0.001. 5 months: control, n=4; CSE, n=4, P<0.05; *Figure 3*), with the corresponding levels in whole lung declining after exposures of 3 months (control, n=4; CSE, n=4, P<0.05) and 5 months (control, n=4; CSE, n=5, P<0.05; *Figure 3F-H*). Mature and precursor BMP4 protein levels related to α-actin in endothelium-denuded PAs were upregulated significantly after smoking exposures of 3 and 5 months compared with the control (3 months: control, n=4; CSE, n= 5; both precursor and mature BMP4, P<0.05; 5 months: control, n=4; CSE, n=4; precursor BMP4, P<0.05, mature BMP4, P<0.001; *Figure 4*). The same trends were seen in whole lung (3 months: control, n=4; CSE, n=4; precursor BMP4, P<0.001, mature BMP4, P<0.05; 5 months: control, n=4; CSE, n=5; both precursor and mature BMP4, P<0.001; *Figure 4G-J*). In addition, the expression of BMPRII was markedly enhanced in the PAs of rats subjected to CSE for 5 months (control, n=4; CSE, n=4, P<0.05; *Figure 5*), while there was no significant alteration of BMPRII expression in whole lung (*Figure 5E-H*). In summary, CSE had opposite effects on BMP4 and PPAR-γ, with the former being elevated and the latter lowered. The augmented expression of BMP4 might contribute to the upregulation of BMPRII.

Smoking exposures of 3 and 5 months markedly enhanced TRPC1 expression in the PA (3 months: control n=4; CSE n=5, P<0.05. 5 months: control n=4; CSE n=5, P<0.05; *Figure 6*); smoking exposure of 1, 3 and 5 months significantly increased TRPC1 expression in whole lung (1 month: control n=4; CSE n=4, P<0.05. 3 months: control n=4; CSE n=4, P<0.05. 5 months: control n=4; CSE n=5, P<0.05; *Figure 6E-H*). TRPC4 protein levels in the PA were upregulated after smoking exposure of 1 month (control, n=4; CSE, n=4, P<0.05), 3 months (control, n=4; CSE, n=5, P<0.05) and 5 months (control, n=4; CSE, n=4, P<0.05; *Figure* 7), although TRPC4 expression in whole lung was significantly enhanced only after smoking exposure of 5 months (control, n=4; CSE, n=4, P<0.001; *Figure 7G-H*). TRPC6 expression in the PA increased considerably after smoking exposure of 3 and 5 months (3 months: control, n=4; CSE, n=5, P<0.05. 5 months: control, n=4; CSE, n=5, P<0.001; *Figure 8*), and the corresponding levels in whole lung were enhanced after smoking exposure of 1 month (control, n=4: CSE, n=4, P<0.05), 3 months (control, n=4; CSE, n=5, P<0.05), and 5 months (control, n=4; CSE, n=5, P<0.001; *Figure 8E-H*).

Discussion

PAH is an important complication of COPD and an independent risk factor that affects the course of COPD. Studies on smoking patients with mild COPD have demonstrated that 25% have slow-progressive increases in pulmonary arterial pressure (32,33). Smoking is one of the main causes of COPD and PAH, but the specific mechanism by which CSE causes chronic PAH is still unclear.

This research presents evidence suggesting that PPAR-γ and BMP4 function as upstream [Ca^{2+}]i regulators in the PAs of rats exposed to cigarette smoke. First, PPAR-γ expression was found to be inhibited in the PAs and whole lungs of CSE rats, suggesting that during cigarette-smoke-induced PAH, this anti-inflammatory biomarker became dysfunctional, and the defect is at the level of PPAR-γ gene expression. Second, we found that (1) cigarette smoke exposure upregulated BMP4 and TRPC expression not only in PAs but also in the whole lung and (2) cigarette smoke induced inflammatory responses in whole lung as consequences of vascular remodeling. According to Floyd *et al*. (30), there was no doubt that persistent vasoconstriction was induced by increased [Ca^{2+}]i. Moreover, Lu *et al*. (13) demonstrated that calcium signaling in PASMCs is regulated by BMP4, probably via upregulated TRPC expression; the latter increases SOCE and basal [Ca^{2+}]i in PASMCs, and thus promotes pulmonary

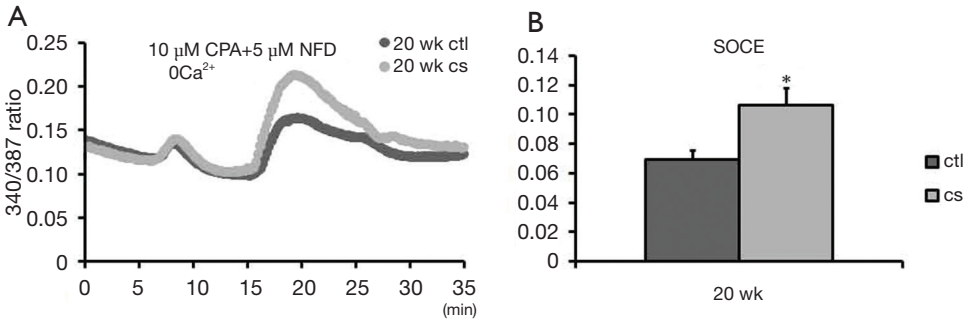

Figure 2 Alterations in $[Ca^{2+}]i$ expression in distal PASMCs of rats exposed to air or cigarette smoke for 20 weeks. (A) Time courses of $[Ca^{2+}]i$ measured by 340/387 ratio before and after restoration of extracellular Ca^{2+} in distal PASMCs perfused with Ca^{2+}-free Krebs-Ringer bicarbonate (KRB) solution containing 10 μM cyclopiazonic acid (CPA), 0.5 mM EGTA, and 5 μM nifedipine (NFD; control, n=5 experiments in 57 cells; CSE, n=5 experiments in 87 cells); (B) statistical analysis of SOCE in (A). *, P value <0.05.

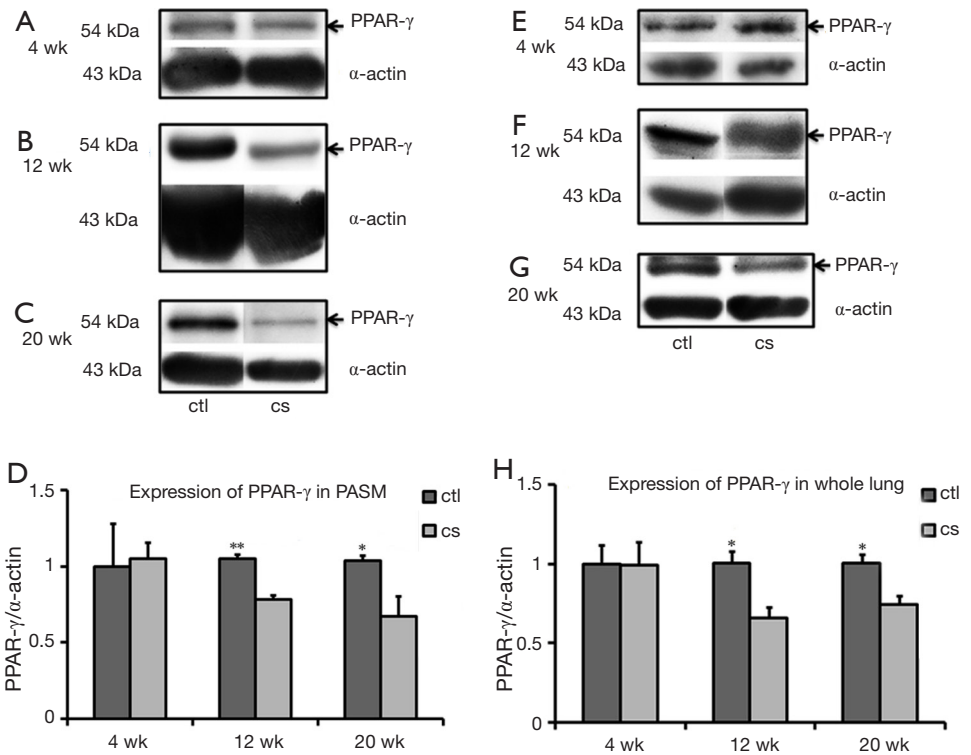

Figure 3 Alterations in PPAR-γ expression in PAs and whole lungs from rats exposed to air or 4/12/20 weeks of cigarette smoke. (A-C) Representative western blots of PPAR-γ proteins in PAs of control and CSE rats; (D) quantitative analysis of PPAR-γ proteins in PAs (4-week control, n=4, 4-week CSE, n=5; 12-week control, n=4, 12-week CSE, n=5; 20-week control and CSE, n=4); (E-G) representative western blots of PPAR-γ proteins in whole lungs from control and CSE rats; (H) quantitative analysis of PPAR-γ proteins in whole lungs (4-week control, n=4, 4-week CSE, n=5; 12-week control, n=4, 12-week CSE, n=4; 20-week control, n=4, 20-week CSE, n=5). Equal protein loading was confirmed using α-actin. PA indicates pulmonary artery. *, P value <0.05; **, P value <0.001.

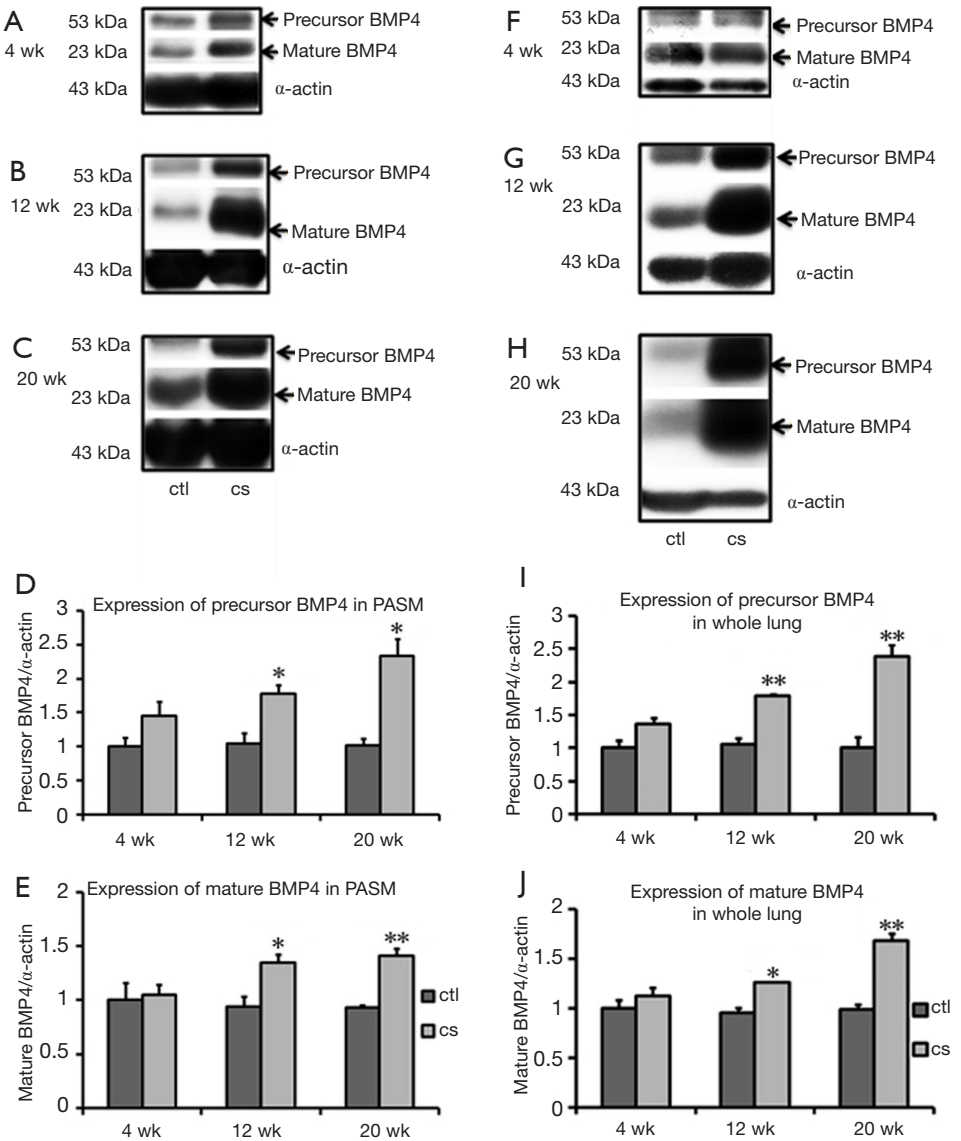

Figure 4 Alterations in BMP4 expression in PAs and whole lungs from rats exposed to air or 4/12/20 weeks cigarette smoke. (A-C) Representative western blots of BMP4 proteins in the PAs of control and CSE rats; (D,E) quantitative analyses of precursor and mature BMP4 proteins in PAs (4-week control, n=4, 4-week CSE, n=5; 12-week control, n=4, 12-week CSE, n=5; 20-week control and CSE, n=4); (F-H) representative western blots of BMP4 proteins in whole lungs of control and CSE rats; (I,J) quantitative analyses of precursor and mature BMP4 proteins in whole lungs (4-week control, n=3, 4-week CSE, n=4; 12-week control and CSE, n=4; 20-week control, n=4, 20-week CSE, n=5). *, P value <0.05; **, P value <0.001.

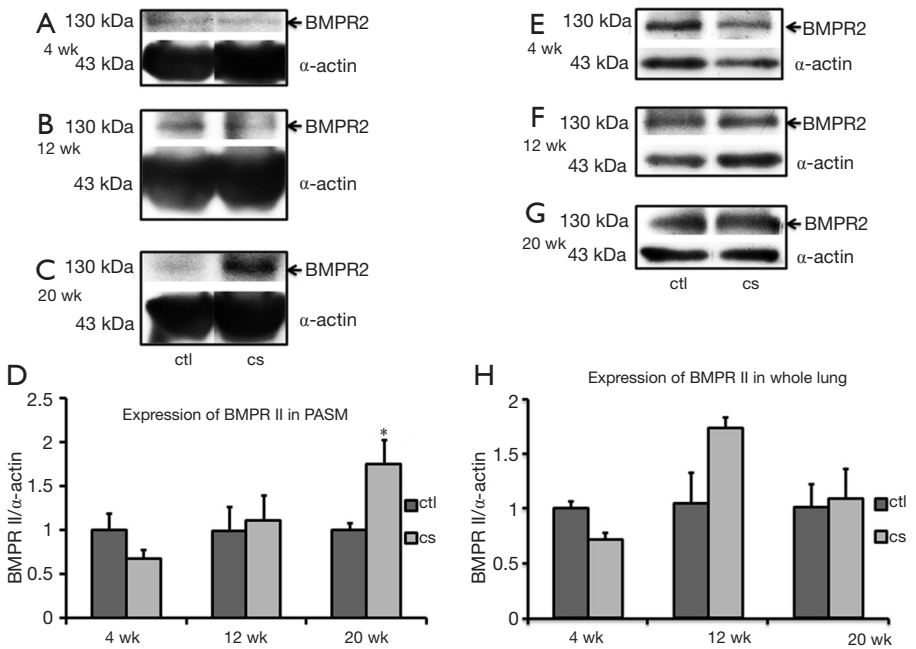

Figure 5 Alterations in BMPR2 expression in PAs and whole lungs from rats exposed to air or 4/12/20 weeks of cigarette smoke. (A-C) Representative western blots of BMPR2 proteins in PAs of control and CSE rats; (D) quantitative analysis of BMPR2 proteins in PAs (4-week control and CSE, n=4; 12-week control, n=4, 12-week CSE, n=5; 20-week control and CSE, n=4); (E-G) representative western blots of BMPR2 proteins in whole lungs of control and CSE rats; (H) quantitative analysis of BMPR2 proteins in whole lungs (4-week control, n=3, 4-week CSE, n=4; 12-week control, n=4, 12-week CSE, n=3; 20-week control, n=4, 20-week CSE, n=5). *, P value <0.05.

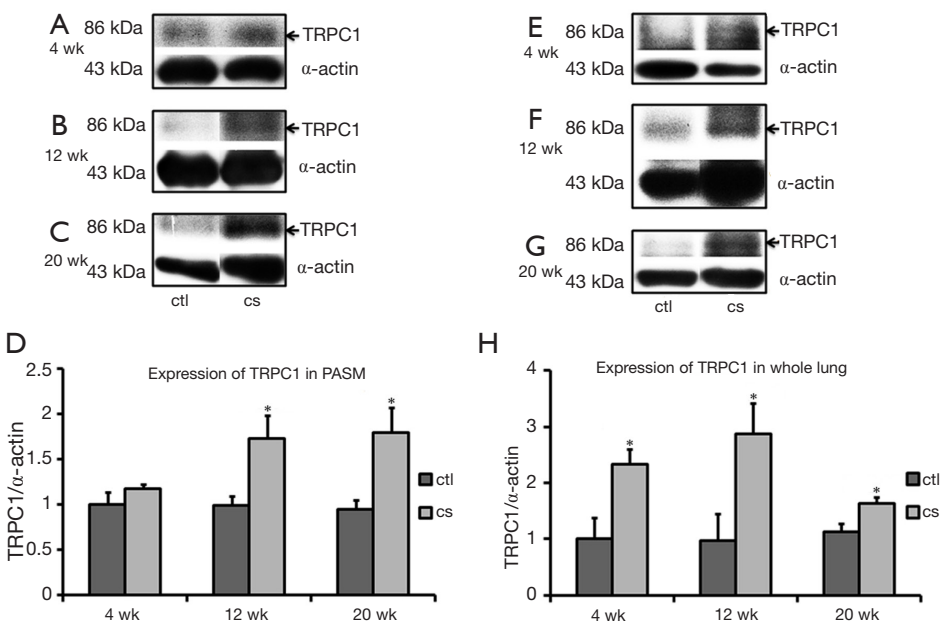

Figure 6 Alterations in TRPC1 expression in PAs and whole lungs from rats exposed to air or 4/12/20 weeks cigarette smoke. (A-C) Representative western blots of TRPC1 proteins in PAs of control and CSE rats; (D) quantitative analysis of TRPC1 proteins in PAs (4-week control, n=4, 4-week CSE, n=5; 12-week control, n=4, 12-week CSE, n=5; 20-week control, n=4, 20-week CSE, n=5); (E-G) representative western blots of TRPC1 proteins in whole lungs of control and CSE rats; (H) quantitative analysis of TRPC1 proteins in whole lungs (4-week control and CSE, n=4; 12-week control and CSE, n=4; 20-week control, n=4, 20-week CSE, n=5). *, P value <0.05.

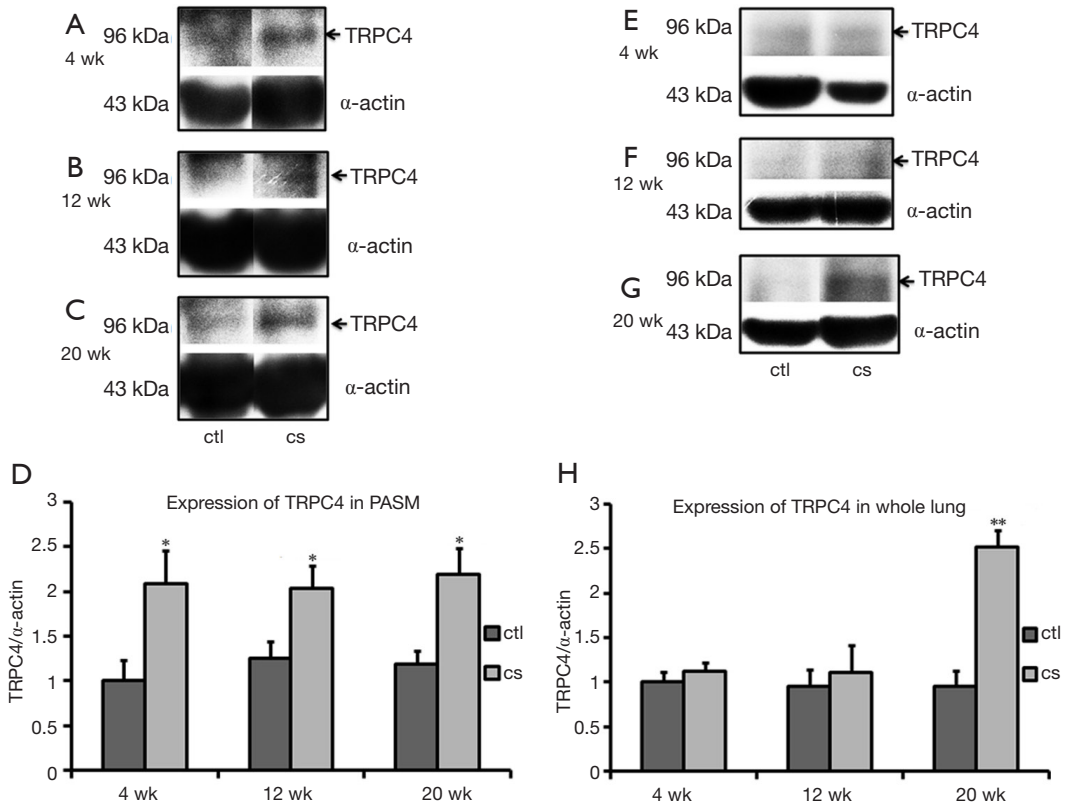

Figure 7 Alterations in TRPC4 expression in PAs and whole lungs from rats exposed to air or 4/12/20 weeks cigarette smoke. (A-C) Representative western blots of TRPC4 proteins in PAs from control and CSE rats; (D) quantitative analysis of TRPC4 proteins in PAs (4-week control and CSE, n=4; 12-week control, n=4, 12-week CSE, n=5; 20-week control and CSE, n=4); (E-G) representative western blots of TRPC4 proteins in whole lungs of control and CSE rats; (H) quantitative analysis of TRPC4 proteins in whole lungs (4-week control, n=4, 4-week CSE, n=5; 12-week control and CSE, n=4; 20-week control and CSE, n=4). *, P value <0.05; **, P value <0.001.

vascular remodeling during PAH. Last, our findings suggest that augmented BMP4 expression may contribute to the enhanced expression of BMPR2.

In conclusion, we found that cigarette smoke upregulates TRPC1, TRPC4, and TRPC6 expression in pulmonary arteries, probably by promoting BMP4 expression. This leads to increased SOCE, which plays a prominent role in dose-dependent vascular remodeling. Augmented expression of BMP4 in the whole lung contributes to inflammatory responses, and BMP4 may also interact with PPAR-γ under normal physiological conditions, thus establishing a barrier to inflammatory responses.

We propose that the downregulation of PPAR-γ and upregulation of BMP4 is crucial in enhanced SOCE, following the upregulation of TRPC1/4/6 in the PAs and lungs of smoking-exposed rats. These changes in PPAR-γ and BMP4 expression also play a part in stimulating inflammatory responses that lead to vascular remodeling. PPAR-γ, expressed in both alveolar macrophages and neutrophils, plays an anti-inflammatory role, and is involved in macrophage activation (34-36).

Acknowledgements

Funding: This study was supported by the National Natural Science Foundation of China (Grant Numbers 81200038, 81173112, and 81170052), the Foundation for Young Talents of Guangzhou Education Bureau (Grant Number 10A152).

Author's contributions: Lei Zhao and Jian Wang initiated the project, designed the experiments, analyzed the data, and drafted and revised the paper. Lei Zhao, Yu-Ting Liang and Wen-Liang Zhou contributed to the animal, functional, and molecular experiments. Yu-Qin Chen and Wen-Jun Lu contributed to the cellular and molecular

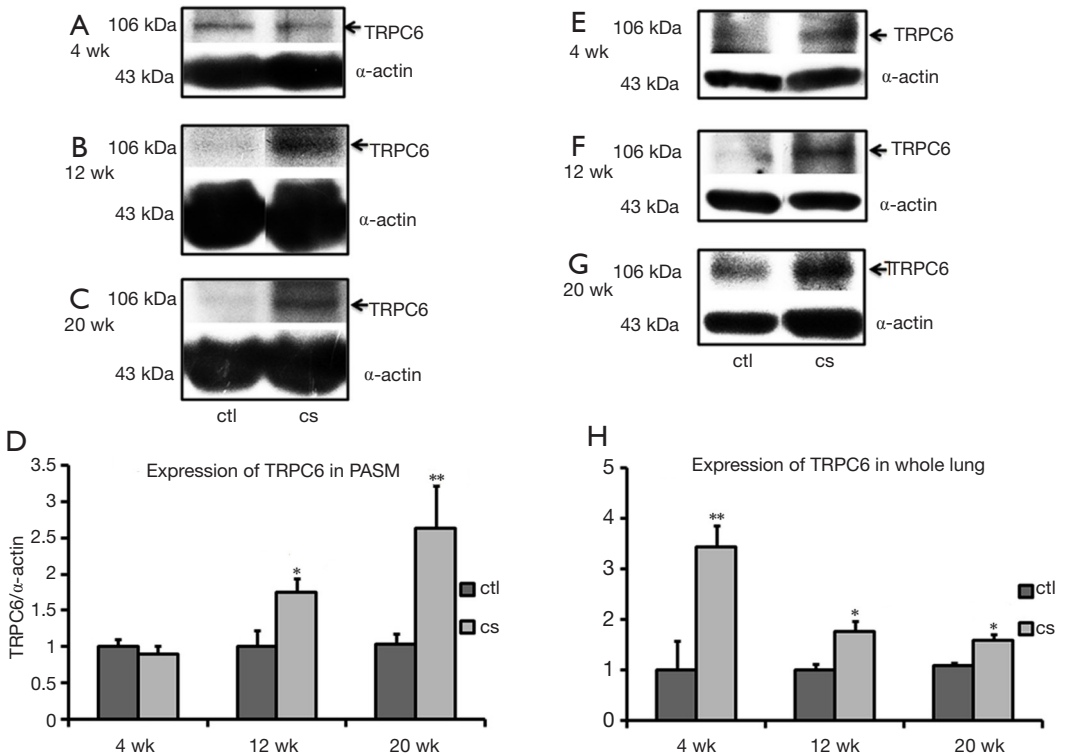

Figure 8 Alterations in TRPC6 expression in PAs and whole lungs from rats exposed to air or 4/12/20 weeks cigarette smoke. (A-C) Representative western blots of TRPC6 proteins in PAs from control and CSE rats; (D) quantitative analysis of TRPC6 proteins in PAs (4-week control, n=4, 4-week CSE, n=5; 12-week control, n=4, 12-week CSE, n=5; 20-week control and CSE, n=4); (E-G) representative western blots of TRPC6 proteins in whole lungs from control and CSE rats; (H) quantitative analysis of TRPC6 proteins in whole lungs (4-week control and CSE, n=4; 12-week control, n=4, 12-week CSE, n=5; 20-week control, n=4, 20-week CSE, n=5). *, P value <0.05; **, P value <0.001.

experiments.

Disclosure: The authors declare no conflict of interest.

References

1. Essop MR. Contemporary insights into the pathogenesis, diagnosis and therapy of pulmonary arterial hypertension. Cardiovasc J Afr 2010;21:334-7.
2. Gomberg-Maitland M. Learning to pair therapies and the expanding matrix for pulmonary arterial hypertension: Is more better? Eur Respir J 2006;28:683-6.
3. Chaouat A, Naeije R, Weitzenblum E. Pulmonary hypertension in COPD. Eur Respir J 2008;32:1371-85.
4. Wright JL, Tai H, Wang R, et al. Cigarette smoke upregulates pulmonary vascular matrix metalloproteinases via TNF-alpha signaling. Am J Physiol Lung Cell Mol Physiol 2007;292:L125-33.
5. Miriyala S, Gongora Nieto MC, Mingone C, et al. Bone morphogenic protein-4 induces hypertension in mice: role of noggin, vascular NADPH oxidases, and impaired vasorelaxation. Circulation 2006;113:2818-25.
6. Tian XY, Yung LH, Wong WT, et al. Bone morphogenic protein-4 induces endothelial cell apoptosis through oxidative stress-dependent p38MAPK and JNK pathway. J Mol Cell Cardiol 2012;52:237-44.
7. Chang K, Weiss D, Suo J, et al. Bone morphogenic protein antagonists are coexpressed with bone morphogenic protein 4 in endothelial cells exposed to unstable flow in vitro in mouse aortas and in human coronary arteries: role of bone morphogenic protein antagonists in inflammation and atherosclerosis. Circulation 2007;116:1258-66.
8. Canalis E, Pash J, Varghese S. Skeletal growth factors. Crit Rev Eukaryot Gene Expr 1993;3:155-66.
9. Reddi AH. Role of morphogenetic proteins in skeletal tissue engineering and regeneration. Nat Biotechnol 1998;16:247-52.
10. Wozney JM, Rosen V, Celeste AJ, et al. Novel regulators of bone formation: molecular clones and activities. Science 1988;242:1528-34.
11. Yamashita H, Ten Dijke P, Heldin CH, et al. Bone

morphogenetic protein receptors. Bone 1996;19:569-74.
12. Takano M, Otsuka F, Matsumoto Y, et al. Peroxisome proliferator-activated receptor activity is involved in the osteoblastic differentiation regulated by bone morphogenetic proteins and tumor necrosis factor-α. Mol Cell Endocrinol 2012;348:224-32.
13. Lu W, Ran P, Zhang D, et al. Bone morphogenetic protein 4 enhances canonical transient receptor potential expression, store-operated Ca2+ entry, and basal [Ca2+]i in rat distal pulmonary arterial smooth muscle cells. Am J Physiol Cell Physiol 2010;299:C1370-8.
14. Xu SZ, Beech DJ. TrpC1 is a membrane-spanning subunit of store-operated Ca(2+) channels in native vascular smooth muscle cells. Circ Res 2001;88:84-7.
15. Beech DJ, Xu SZ, McHugh D, et al. TRPC1 store-operated cationic channel subunit. Cell Calcium 2003;33:433-40.
16. Bergdahl A, Gomez MF, Dreja K, et al. Cholesterol depletion impairs vascular reactivity to endothelin-1 by reducing store-operated Ca2+ entry dependent on TRPC1. Circ Res 2003;93:839-47.
17. Dietrich A, Chubanov V, Kalwa H, et al. Cation channels of the transient receptor potential superfamily: their role in physiological and pathophysiological processes of smooth muscle cells. Pharmacol Ther 2006;112:744-60.
18. Wang J, Shimoda LA, Sylvester JT. Capacitative calcium entry and TRPC channel proteins are expressed in rat distal pulmonary arterial smooth muscle. Am J Physiol Lung Cell Mol Physiol 2004;286:L848-58.
19. Dietrich A, Mederos y Schnitzler M, Kalwa H, et al. Functional characterization and physiological relevance of the TRPC3/6/7 subfamily of cation channels. Naunyn Schmiedebergs Arch Pharmacol 2005;371:257-65.
20. Dietrich A, Mederos Y, Schnitzler M, et al. Increased vascular smooth muscle contractility in TRPC6-/- mice. Mol Cell Biol 2005;25:6980-9.
21. Firth AL, Remillard CV, Yuan JX. TRP channels in hypertension. Biochim Biophys Acta 2007;1772:895-906.
22. Zhang S, Remillard CV, Fantozzi I, et al. ATP-induced mitogenesis is mediated by cyclic AMP response element-binding protein-enhanced TRPC4 expression and activity in human pulmonary artery smooth muscle cells. Am J Physiol Cell Physiol 2004;287:C1192-201.
23. Ng LC, Gurney AM. Store-operated channels mediate Ca(2+) influx and contraction in rat pulmonary artery. Circ Res 2001;89:923-9.
24. Liu XR, Zhang MF, Yang N, et al. Enhanced store-operated Ca^{2}+ entry and TRPC channel expression in pulmonary arteries of monocrotaline-induced pulmonary hypertensive rats. Am J Physiol Cell Physiol 2012;302:C77-87.
25. Nadziejko C, Fang K, Bravo A, et al. Susceptibility to pulmonary hypertension in inbred strains of mice exposed to cigarette smoke. J Appl Physiol (1985) 2007;102:1780-5.
26. Yamato H, Sun JP, Churg A, et al. Guinea pig pulmonary hypertension caused by cigarette smoke cannot be explained by capillary bed destruction. J Appl Physiol (1985) 1997;82:1644-53.
27. Wright JL, Tai H, Churg A. Vasoactive mediators and pulmonary hypertension after cigarette smoke exposure in the guinea pig. J Appl Physiol (1985) 2006;100:672-8.
28. Satoh K, Matoba T, Suzuki J, et al. Cyclophilin A mediates vascular remodeling by promoting inflammation and vascular smooth muscle cell proliferation. Circulation 2008;117:3088-98.
29. Lu W, Wang J, Peng G, et al. Knockdown of stromal interaction molecule 1 attenuates store-operated Ca2+ entry and Ca2+ responses to acute hypoxia in pulmonary arterial smooth muscle. Am J Physiol Lung Cell Mol Physiol 2009;297:L17-25.
30. Floyd R, Wray S. Calcium transporters and signalling in smooth muscles. Cell Calcium 2007;42:467-76.
31. Wang J, Weigand L, Wang W, et al. Chronic hypoxia inhibits Kv channel gene expression in rat distal pulmonary artery. Am J Physiol Lung Cell Mol Physiol 2005;288:L1049-58.
32. Kessler R, Faller M, Weitzenblum E, et al. "Natural history" of pulmonary hypertension in a series of 131 patients with chronic obstructive lung disease. Am J Respir Crit Care Med 2001;164:219-24.
33. Scharf SM, Iqbal M, Keller C, et al. Hemodynamic characterization of patients with severe emphysema. Am J Respir Crit Care Med 2002;166:314-22.
34. Szatmari I, Nagy L. Nuclear receptor signalling in dendritic cells connects lipids, the genome and immune function. EMBO J 2008;27:2353-62.
35. Penyige A, Poliska S, Csanky E, et al. Analyses of association between PPAR gamma and EPHX1 polymorphisms and susceptibility to COPD in a Hungarian cohort, a case-control study. BMC Med Genet 2010;11:152.
36. Standiford TJ, Keshamouni VG, Reddy RC. Peroxisome proliferator-activated receptor-{gamma} as a regulator of lung inflammation and repair. Proc Am Thorac Soc 2005;2:226-31.

Cite this article as: Zhao L, Wang J, Wang L, Liang YT, Chen YQ, Lu WJ, Zhou WL. Remodeling of rat pulmonary artery induced by chronic smoking exposure. J Thorac Dis 2014;6(6):818-828. doi: 10.3978/j.issn.2072-1439.2014.03.31